ARMA 11-584

The Analysis of Stress Tensor Determined from Seismic Moment Tensor Solutions at Goldex Mine, Quebec

Trifu, C-I. and Shumila, V.
ESG Inc., Kingston, Ontario, Canada

This paper was prepared for presentation at the 45th US Rock Mechanics / Geomechanics Symposium held in San Francisco, CA, June 26–29, 2011.

ABSTRACT: Mine models incorporate geological, geotechnical, and rock mechanics principles to offer a 3D distribution of the principal stresses within the rockmass. Information that can independently confirm and calibrate these models is essential to offer reliable tools to the industry. Event mechanisms have long been used in earthquake seismology to infer the orientation of principal stresses assuming quasi-static stresses. This study evaluates the conditions under which the stress tensor can be derived from event mechanisms in a mining environment. Advantage is taken of the microseismic array at Goldex mine, Quebec. The array comprises 4 triaxial and 22 uniaxial accelerometers covering a volume of 450 x 250 x 120 m. A total of 544 reliable seismic moment tensor solutions for events occurred between February and May 2009 are retained for analysis. The results indicate that the mechanism solutions exhibit a high variability in both the type of fracture components and the actual fault-plane geometry. The most significant clustering of these solutions appears related to the development blasts. These blasts cause a significant reorientation of the stress tensor in a volume adjacent to that of the advancing cave front. It is further shown that the highest homogeneity in the orientation of the moment tensor solutions is obtained for events closely located in time and space with respect to each other.

1. INTRODUCTION

Underground mine design and development rely heavily of the modeling of the stress distribution and redistribution within the rock mass. Mine operations change rapidly the underground conditions, and implementing changes to the mine model is often far from trivial, requiring time. Meanwhile, direct stress measurement data is very limited, making difficult an independent testing and evaluation of the mine model proposed by rock mechanics.

The seismic moment tensor (SMT) provides the orientations of the principal strain axes, which are related to the local ST components (magnitudes and orientations) through the Hook's law. In earthquake seismology, stress tensor (ST) inversion based on fault-plane orientations obtained from seismic moment tensor (SMT) solutions was pioneered by [1]. He demonstrated that the only constraint imposed on ST orientation by a fault-plane solution is that the largest principal ST axis lies in the quadrant defined by pressure (P) axis of the SMT. Some seismological studies use an average P-axis direction as equivalent to the direction of the largest principal stress.

Formal algorithms for ST inversions were developed by [2, 3]. The most recent algorithm, based on a Bayesian approach to ST inversion, was introduced by [4]. Despite the long development history of ST inversion from seismological data, it remains work in progress. This is due to the intrinsic ambiguity of fault-plane solutions obtained from SMT inversions, as well as to the assumption of uniform (quasi-static) ambient stress field within the volume or region where the SMT data set was collected.

ST inversion of SMT solutions for mining induced seismicity is even more challenging. In the mining environment, along with problems mentioned above, conventional assumptions, like the main and intermediate ST or SMT principal axes pointing downward [4] are not obvious. Almost all ST inversion algorithms make such assumptions based on the fact that SMT data come from surface observations of sources at depth, were stress is often dominated by the lithostatic pressure. Microseismic monitoring in mines is based on three dimensional arrays and the *a priori* orientation of the ST axes could be arbitrary. Moreover, while earthquake sources exhibit pure shear failures, mine seismicity includes a large range of fracture components.

Seismicity in mines highlights the zones were stress yielding conditions occur. Thus, microseismic

monitoring provides indirect information on the stress distribution underground. Source parameters such as magnitude, energy release, size, apparent or static stress drop allow for approximate assessment of possible ranges of acting stress magnitudes. Furthermore, seismic waveform inversion for failure mechanisms or SMT solutions provides means to evaluate directly the principal stress orientations and relative stress magnitudes.

The present study is a preliminary work intended to evaluate the conditions under which ST inversions can be carried out on SMT solutions derived from mine seismic events using the algorithm proposed in [4]. Once these conditions can be established, reliable inversions can be made available for practical use.

2. STRESS INVERSION

Under The stress inversion attempts to determine four model parameters - three Euler angles, which define the orientation of the principal stresses, and the relative stress magnitudes ratio $R=(\sigma_1-\sigma_2)/(\sigma_1-\sigma_3)$. The resulting principal stress tensor will be the one that is capable to generate strain tensors at event locations which best fit the observations represented by SMT inversions. The measure of misfit depends on the approach employed. In case of [2] for example, the misfit is the sum of angles between the observed slip direction and shear vector of the stress tensor model, or the sum of some increasing function of those angles. This is generalized in [3], where the misfit is the sum of angles required to rotate the stress model into each of the observed mechanism solutions. Accounting for prime vs. auxiliary plane ambiguity is done by selecting the smallest angle of rotation for each solution. Only rotations which provide acceptable range for stress shape factor $0 \leq R \leq 1$, and correct shear stress direction vs. direction of the slip vector are taken into account.

The approach in [4] employs a Bayesian framework in the ST inversion problem. The misfit is measured by the probability of a given stress model conditioned on an obtained set of observations. In the absence of any additional information, a uniform probability distribution function over the entire parameter space is adopted as *a priori* distribution. For rotation matrices under consideration, a suitable misfit generation mechanism is represented by a Fisher matrix distribution. The likelihood of a fault-plane solution for a stress model can be defined as a function of a precision coefficient - analogues of inverse standard deviation for a Gaussian distribution. Worth noting, the assuming statistical independence of observations, the likelihood function that accounts for auxiliary and prime fault plane ambiguity is equal, which means that both planes are assumed to be equally probable.

Alternatively, the precision coefficient can be defined as a function of the standard deviation of fault-plane orientation angle estimates. For example, angle precisions of 1, 5, 10, and 20° would correspond to values of 1000, 60, 17, and 5 [4]. The distribution of ST model parameters is found by integrating the likelihood function over all possible orientations of the fault-plane solutions. The integral can be tabulated for a number of solutions, after which the value for any other particular solution is found by interpolation.

Practical implementation of the approaches described in [3] and [4] involves direct grid search over possible stress tensor orientations and factor shapes. In case of the former approach, however, the algorithm starts with a pre-defined orientation of the stress tensor major principal axis and operates over a grid around that initial direction, while the latter approach explores all possible spatial orientations. Fisher matrix probability distribution suggests a standard, direct maximum likelihood approach. In this case the precision coefficient can be interpreted as a weighting function for each mechanism solution. This weighting could be a value inversely proportional to the respective conditional number, or any other quantitative measure provided by the inversion algorithm.

3. SEISMICITY AT GOLDEX MINE AND SENSOR ARRAY PERFORMANCE

Goldex is a gold mine near Val d'Or, in northwestern Quebec. The ore body is 750 m below surface, with the geology oriented 280°N and dipping 75-85° to the North. Small diorite dykes cut the ore body at almost perpendicular angle. The overall rock mass quality is very high, reason why a novel open stope mining method, called long-hole shrinkage, was developed and employed [5]. The seismic array includes 4 triaxial and 22 uniaxial accelerometers at 20 kHz sampling (Fig. 1). Fiber optic cables are used for data acquisition on a surface PC, and GPS time synchronization.

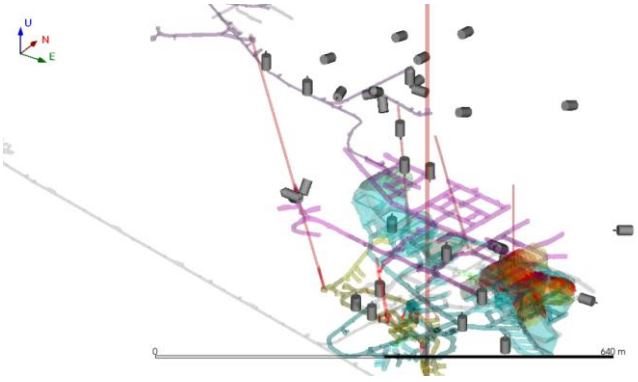

Fig. 1. Microseismic monitoring array at Goldex mine. Gray cylinders show the sensor locations.

Seismic array provides an exceptional coverage of a 450 x 250 x 120 m volume of interest. Indeed, automatic event location accuracy exceeds 10 m for only about 1% of seismicity, and can be improved further through manual processing. The ability of the array geometry to offer reliable source mechanism solutions can be evaluated through the conditional number [6] at 3D grid points within the respective volume. As shown in Fig. 2, high quality SMT inversions can be expected around both the West and East Stopes.

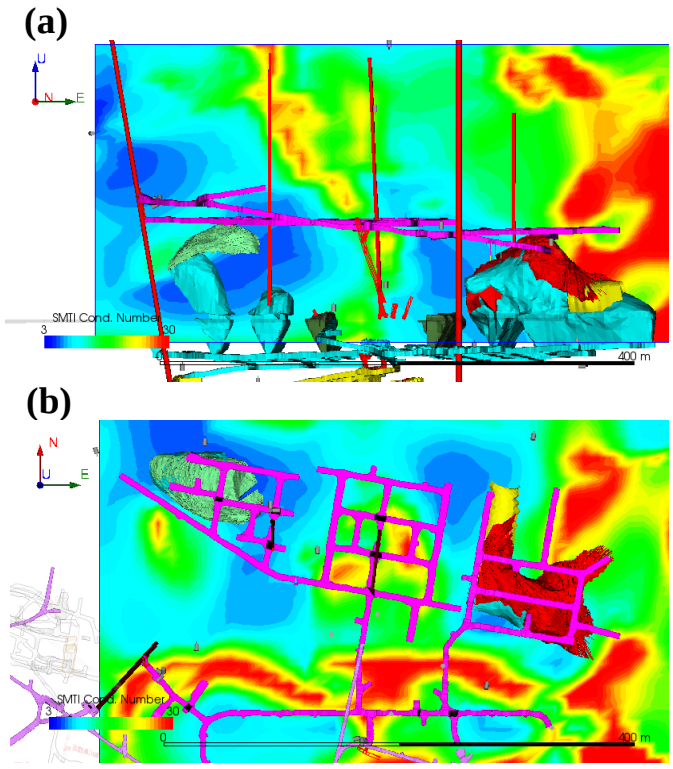

Fig. 2. Conditional number for SMT inversions, calculated over the study volume at 3D grid points in (a) north-east and (b) east-depth projections.

4. DATA ANALYSIS

On-line far-field low-frequency spectral level estimates with first polarities attached, recorded at both triaxial and uniaxial sensors are employed in SMT inversions [7, 8]. To a first approximation, uniform P- and S-wave velocities were used as determined from calibration blasts: 6180 and 3640 m/s, respectively.

The analysis will concentrate on a set of 978 events occurred between February 2 and May 30, 2009 and located around the East Stope, underlining nicely the cave front (Fig. 3). Automatic processing led to a combined set of mechanism solutions of variable quality. For further analysis, only solutions based on at least 18 observations, with correlation coefficient higher than 0.6 and Conditional Number less than 15 were retained, resulting in a subset of 544 solutions.

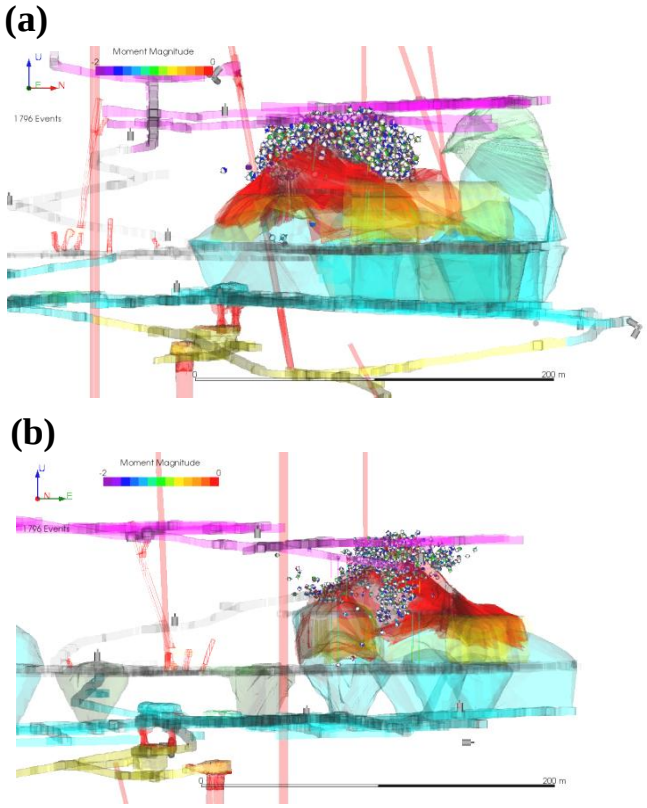

Fig. 3. Microseismic events with SMT solutions are located around the East Stope in (a) north-depth and (b) east-depth projections.

The results are presented in Fig. 4a on a source mechanism type diagram [9]. Solutions exhibit a large variety of mechanisms that depart from the simple pure-shear or double-couple model. Major double-couple geometry is shown in Fig. 4b on a faulting type diagram [10], which reveals a slight dominance of the vertical strike-slip events.

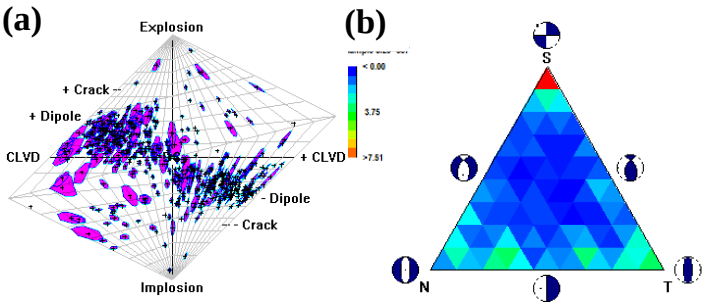

Fig. 4. Event mechanisms for the events around the East Stope on source mechanism (a) and faulting (b) type diagrams. Contours surrounding data points (crosses) in (a) correspond to one sigma interval for the respective estimates.

The distribution of major double-couple P-axes for the SMT solutions corresponding to this subset is shown in Fig. 5, evaluated using adaptive Kernel Density Estimation approach with distance defined as the arc on

the unit sphere. At least four different clusters seem present, characterized by sub-vertical, dipping at 50-70°, and sub-horizontal P-axes at azimuths 0° and 270°.

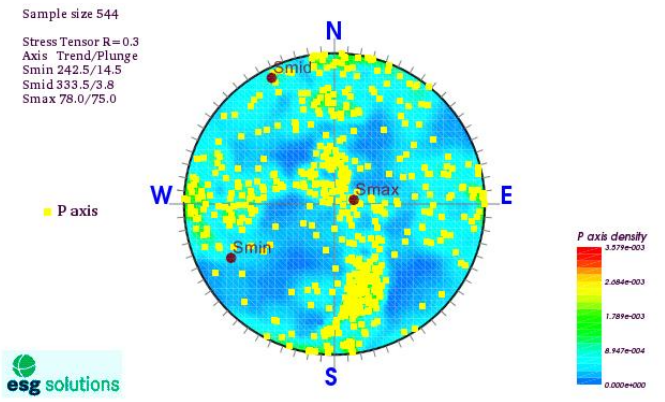

Fig. 5. Distribution of the SMT major double-couple P-axes around the East Stope, and the result of the ST inversion. Color refers to the probability density function.

The number of apparent clusters suggests that the main grouping mechanism is related to three development blasts occurred on April 21, May 14, and May 23, 2009. Under this assumption, the data sample was subdivided in the time intervals listed in Table 1 and the ST inversion was carried out for each cluster separately. The results are summarized in Tables 1 and 2. Except for period related to the May 14 blast, σ_1 orientation remains sub-vertical. However, the inversion results exhibit significant ST rotation from one development blast to another.

Table 1. Stress tensor inversion results for subsets of events related to development blasts.

Time interval	Nr events	R	Principal Axis Azimuth(°)/Dip(°)		
			σ_1	σ_2	σ_3
<Apr 21	127	0.8	235/23	143/5	42/66
Apr 21	231	0.1	301/5	209/17	45/72
May 14	94	0.4	257/30	57/59	162/9
May 23	104	0.1	129/3	39/6	237/81

Knowing the ST orientation and shape coefficient permits the mapping of the most probable fault planes from SMT inversions on a 3D Mohr diagram. An example is shown in Fig. 6 for the data corresponding to the pre-blasting period ending on April 21, 2009. Relative shear and normal stresses are evaluated for most probable of the two possible fault plane solutions for each event. This mapping further allows the evaluation of the slope of the Coulomb failure criterion, which in this case suggests a friction angle of 36°.

Time/Events	P-axis distribution
Before blasts, 127 solutions	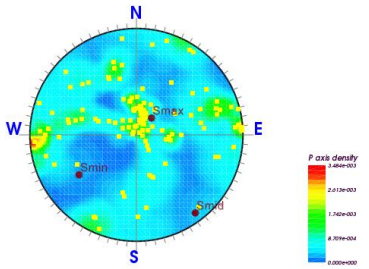
May 14 blast. 94 solutions	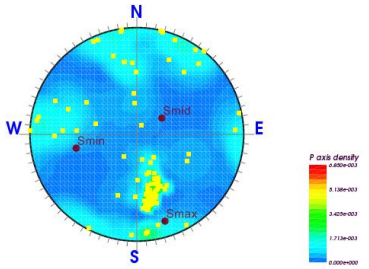
April 21 blast. 231 solutions	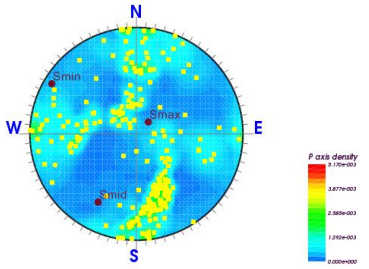
May 23 blast. 104 solutions	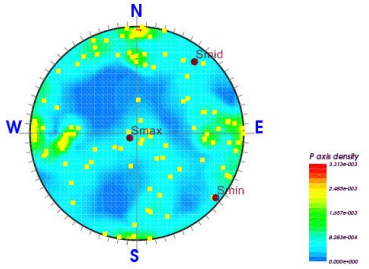

Table 2. SMT P-axis density distribution and ST inversion results related to development blasts.

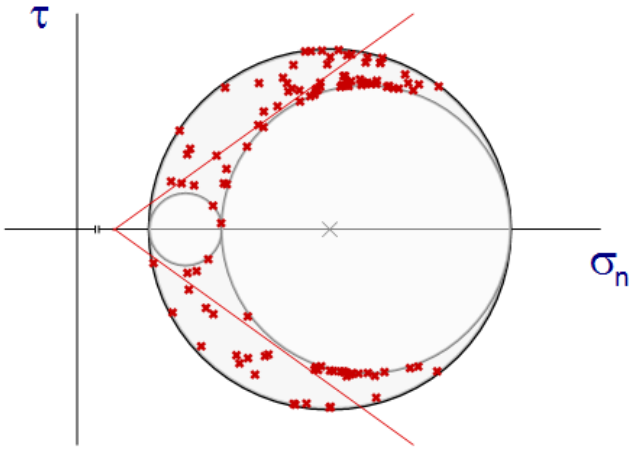

Fig. 6. Scaled Mohr diagram prior to April 21. Thin lines show Coulomb failure envelope with a friction angle of 36°.

5. DISCUSSION

The evaluation of the stress tensor involves a set of hypotheses which are hard to formalize objectively. For example, for some particular fault-plane orientations, the Euler rotation will not work due to effects such as the Gimbals' lock. Such cases are treated in [3] by reassigning vector components to predefined, slightly perturbed values. A more objective treatment is offered in [4], where they are assigned zero likelihood for a particular parameter combination.

However, the most difficult assumption to use is that of the quasi-static stress tensor over the region under consideration for each specific inversion. For the mining environment, theoretical modeling (finite differences or any other numerical method) and microseismic data distributions clearly show that areas of highest interest are those where the stress field exhibits high variability.

There is no formal criterion to evaluate the scale of uniformity hypothesis. Moreover, it can be demonstrated though [11] that stress tensor inversion based on seismological data is subject to high heterogeneity and that uniformity of ambient stress is incompatible with expected low variance of internal friction coefficient (Bayle's law).

Non-uniform stress distribution should be reflected in heterogeneity of SMT solutions. To investigate this effect, Fig. 7a shows the distribution of minimum rotation angle calculated for all pairs of events in the data sample (gray vertical bars) and a subsample of events which are separated by less than 5m. Fig. 7b presents the result the same minimum rotation angle for event pairs separated by less than 24 hours. The results suggest that as the events are located closer in time and space, they tend to be more homogeneous.

6. CONCLUSIONS

Based on a preliminary analysis carried out on a set of 544 seismic events recorded at Golden mine, it can be concluded that SMT solutions exhibit a high variability in the fracture components and the fault-plane geometry. The most significant clustering of SMT orientations appears related to the development blasts. These blasts cause a significant reorientation of the stress tensor in the volume adjacent to the advancing cave front. The highest homogeneity in the orientation of the SMT solutions is obtained for events located closely with respect to each other, both in time and space.

Further research on ST inversion from seismic data should include (i) the development of a more robust, mining specific SMT inversion algorithm, (ii) improved criteria for the spatial-temporal constraint/clustering for ST inversion, as well as (iii) a synthetic, hybrid approach that incorporates not only seismic information but also stress modeling results.

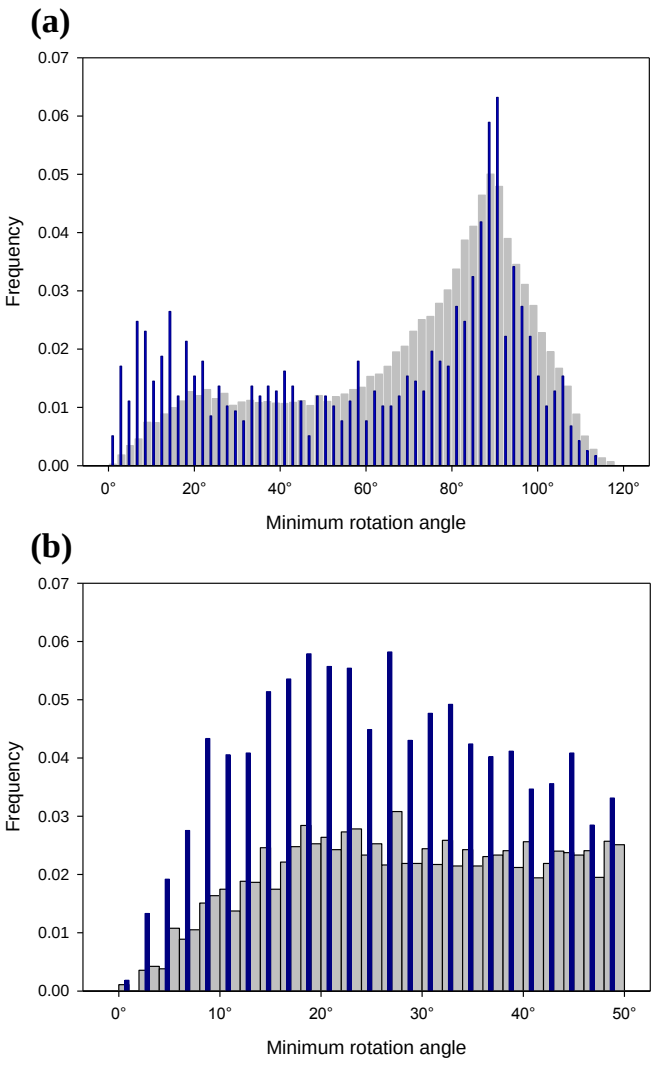

Fig. 7. Distribution of the minimum rotation angle for pair of mechanism solutions. The entire data sample is shown in gray. Dark blue bars correspond to pair events (a) separated by less than 5 m; and (b) separated by less than 24 hours.

REFERENCES

1. McKenzie, D. 1969. The relationship between fault plane solutions for earthquakes and the directions of the principal stresses, *Bull. Seism. Soc. Am.* 59**:** 591–601
2. Angelier, J. 1979. Determination of the mean principal directions of stresses for a given fault population, *Tectonophysics* 56: T17–T26.
3. Gephart, J.W. and D.W. Forsyth. 1984. An improved method for determining the regional stress tensor using earthquake focal mechanism data: application to the San Fernando earthquake sequence. *J. Geophys. Res.* 89: 9305–9320.
4. Arnold, A. and J. Townend. 2007. A Bayesian approach to estimating tectonic stress from seismological data. *Geophys. J. Int.* 170: 1336–1356.

5. Hudyma M.R., P. Frenette, and I. Leslie. 2010. Monitoring Open Stope Caving at Goldex Mine. Australian Centre for Geomechanics, University of Western Australia.

6. Dufumier, H. and L. Rivera. (1997). On resolution of the isotropic component in moment tensor. *Geophys. J. Int.* 131: 595-606.

7. Trifu, C-I., D. Angus, and V. Shumila. (2000). A fast evaluation of the seismic moment tensor for induced seismicity. *Bull. Seismol. Soc. Am.* 90: 1521-1527.

8. Trifu, C-I. and V. Shumila. (2002). Reliability of seismic moment tensor inversions for induced microseismicity at Kidd mine, Ontario. *PAGEOPH* 159: 145-164.

9. Hudson, J.A., R.G. Pearce, and R.M. Rogers. 1989. Source type plot for inversion of the moment tensor. *J. Geophys. Res*. 94: 765-774.

10. Frohlich, C. 2001. Display and quantitative assessment of distributions of earthquake focal mechanisms. *Geophys. J. Int.* 144: 300-308.

11. Rivera, L. and H. Kanamori. 2002. Spatial heterogeneity of tectonic stress and friction in the crust. *Geophys. Res. Lett.* 29.